Magnetic relaxation properties of helium-3 adsorbed on hexagonal boron nitride

T. P. Crane and B. P. Cowan
Millikelvin Laboratory, Royal Holloway University of London, Egham Hill, Egham, Surrey, TW20 0EX, United Kingdom
(Received 31 July 2000)

We present pulse NMR measurements on ^{3}He adsorbed on hexagonal boron nitride powder in the registered phase. We observe strong coupled magnetic relaxation with substrate ^{11}B spins, mediated by ^{14}N surface-layer spins via the level-crossing or quadrupole-dip (QD) effect at 4.5 MHz. *Ab initio* electronic structure calculations of the BN surface-layer electric field gradients, dramatically modified by the ^{3}He were essential in justifying our QD explanation. BN crystallite geometry plays a key role in producing the QD. Stretched exponential fits to the QD relaxation data may provide a new tool for studying specifically the commensurate phases on BN and related materials.

In the study of adsorbed systems over many years, graphite with its smooth, largely fault-free exposed basal planes has proven to be one of the best adsorber materials. It does, however, have some undesirable properties. From the NMR point of view the most serious is its large anisotropic diamagnetic moment which masks dipolar spin-spin relaxation in all but the high coverage, low temperature solid. This has motivated the search for alternative substrates. Hexagonal boron nitride (h-BN) has a very similar structure and lattice dimensions to graphite. BN: $a=b=2.50$ Å, $c=6.66$ Å;[1] graphite: $a=b=2.46$ Å, $c=6.71$ Å.[2] It is also isoelectronic with graphite, having the same strong, short, sp2-hybridized intralayer bonds together with long, weak, interlayer bonds but is an insulator rather than a semimetal. More importantly, the (h-BN) c-axis diamagnetic susceptibility is far smaller: 0.48×10^{-6} emu/gr (Ref. 3) compared with 1.73×10^{-5} emu/gr (Ref. 4) which has permitted the observation of ^{3}He dipolar mediated relaxation effects in the fluid.[5]

The BN powder used in this work was Carborundum Co. HCP SHP-325, the sieve mesh indicating an average particle size of 50 μm. However electron micrographs indicate the crystallites are conglomerates of smaller flat particles with sizes 2–10 μm. Our sample was heat treated to 1000 °C for 24 h to remove impurities and yielded an adsorption area of 80.6 ± 0.6 m^2 from a ^{3}He point-B isotherm of 26.2 ± 0.2 cm^3 gas at STP for a sample mass of 10.58 ± 0.04 g.

Figure 1(a) shows spin-lattice relaxation time T_1 vs coverage at 1 K. In analogy with the phase digram for ^{3}He on graphite we associate the deep dip at $x=0.75$ with the formation of the $\sqrt{3}\times\sqrt{3}R30$ epitaxially registered phase in which one in every three BN hexagons adsorbs a ^{3}He atom. As on graphite, T_1 falls for $x=0.3\rightarrow0.75$ as spins register and exchange motion in the helium film is partially suppressed by the substrate hexagon potential wells. For $x=0.75\rightarrow0.9$ the effect falls-off as the commensurate phase gives way to incommensurate solid.

The frequency dependence of T_1 at $x=0.75$ (Fig. 2), possesses a deep dip located near 4.5 MHz—a feature inexplicable in terms of homonuclear dipolar relaxation, viz.,

$$1/T_1 = J_1(\omega_0) + 4J_2(2\omega_0),$$

where the dipolar spectral functions, $J_n(\omega)$ decay smoothly with frequency ω, ω_0 the Larmor frequency scaling linearly with the applied field. Instead we appeal to coupled dipolar relaxation between ^{3}He spins and a substrate spin species possessing a suitable quadrupole frequency ω_Q, to provide a magnetic relaxation pathway maximally efficient at 4.5 MHz. The heteronuclear, *same-spin* relaxation rate from the Solomon-Bloembergen equations for coupled magnetic relaxation[6]

$$\rho_2 = \tfrac{1}{3}J_0(\omega_x-\omega_y) + J_1(\omega_x) + 2J_2(\omega_x+\omega_y)$$

shows magnetization transport will be most efficient for $\omega_x/2\pi \equiv |\omega_0|/2\pi$ of ^{3}He$=4.5$ MHz when $\omega_y/2\pi \equiv |\omega_Q|/2\pi$ of the substrate nucleus is also 4.5 MHz. This type of level-crossing phenomenon is known as the quadrupole dip[7] and has been extensively reported in proton–quadrupole nucleus bearing molecules, including several containing ^{14}N such as complex organic or biomolecules.[7,8]

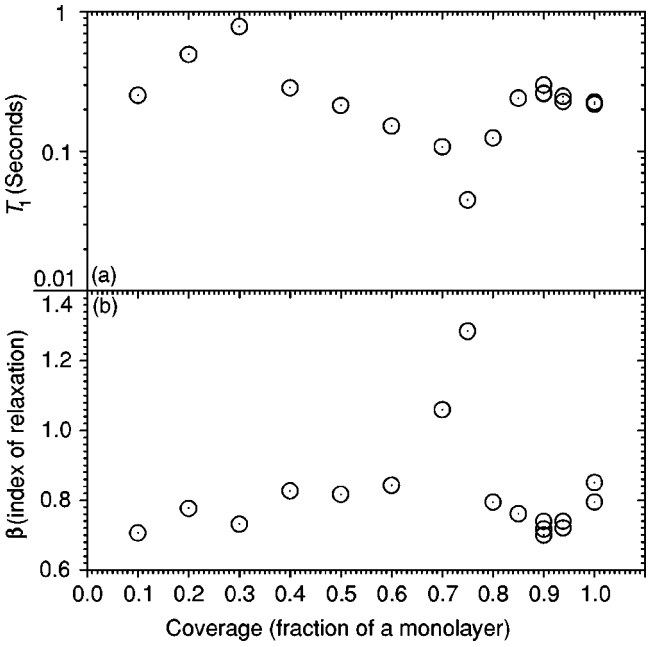

FIG. 1. ^{3}He NMR data as a function of coverage, taken at 1.1 K and 4.5 MHz: (a) T_1, (b) Index of relaxation β.

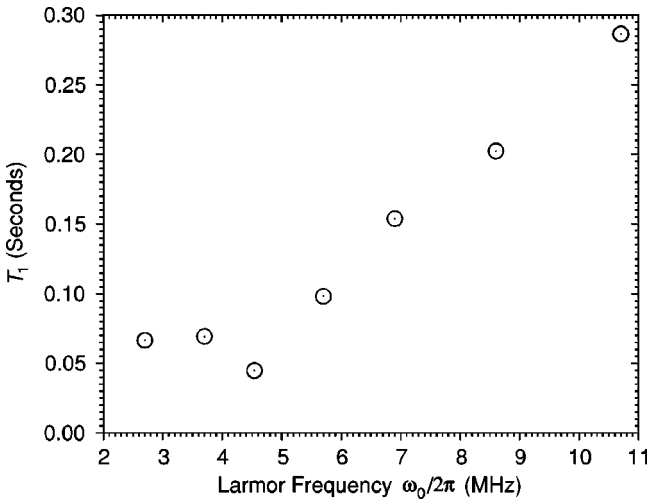

FIG. 2. ^{3}He T_1 as a function of Larmor frequency $\omega_0/2\pi$, taken at 1.1 K and 0.75 monolayers.

A key feature of QD spectroscopy is the mapping of the zero and low-frequency regions of the dipolar spectral functions to higher frequencies where observation is much easier.[9] BN comprises four spin bearing isotopes ^{10}B($I=3$), ^{11}B($I=\frac{3}{2}$), ^{14}N($I=1$), and ^{15}N($I=\frac{1}{2}$) with, respectively, 19.6, 80.4, 99.635, and 0.0635 % relative natural abundances. The key question is: which is responsible for the 4.5 MHz feature?

The ^{11}B quadrupole frequency in *h*-BN has been measured by several different workers, verified in our work and is only 1.47 MHz.[10] Moreover at applied field $4.5\times 2\pi/\gamma_{\mathrm{He}}$, the ^{11}B Larmor frequency is greater than its quadrupole frequency. The low abundance, quadrupole frequencies and large spin I of ^{10}B also make this isotope a poor candidate. This leaves only ^{14}N. The QD has been previously observed in ^{3}He–^{14}N adsorbed systems comprising 1–2 layers of solid N_2.[11] Despite our coarse data grid the width of the broad dip is consistent with Zeeman broadening of the ^{14}N quadrupole line[9] under the powder average where ^{3}He resonant adsorption is smeared over $[\omega_Q \pm \omega_0\gamma_{\mathrm{N}}/\gamma_{\mathrm{He}}]/2\pi \cong 4.5\pm 0.4$ MHz. In addition to the level-crossing, three additional conditions are essential for observation of a QD:[12] (1) $\omega_Q > 1/\tau_c$, where τ_c is a time characteristic of the motion modulating the ^{3}He–^{14}N interaction and puts an upper limit on motional speed, ensuring the dip is not motionally narrowed away. (2) $\omega_Q > \omega_0(^{14}\mathrm{N})$, the ^{14}N Larmor frequency. It sets the limit on Zeeman smearing and is clearly fulfilled here. (3) A fast spin-lattice or other relaxation mechanism to provide a sink for the ^{14}N spin bath. NMR data from the registered phase of ^{3}He on graphite yields $\tau_c \sim 3\times 10^{-8}$ s (Ref. 13) which corresponds to $[\omega_Q \sim 1/\tau_c]/2\pi \sim 5$ MHz. Bearing in mind the sensitivity of quantum exchange motion to substrate related differences, e.g., binding energy, lattice constants, suggests condition (1) is probably only just fulfilled. Support comes from the temperature dependence of T_1 and spin-spin relaxation time T_2 at $x=0.75$ and 4.5 MHz shown in Fig. 3. T_1 falls off strongly at low temperatures as the residual thermal activated vacancy tunneling motion disappears leaving only exchange but T_2 which is also motion dependent is essentially constant at these temperatures because it is dominated by homonuclear processes.

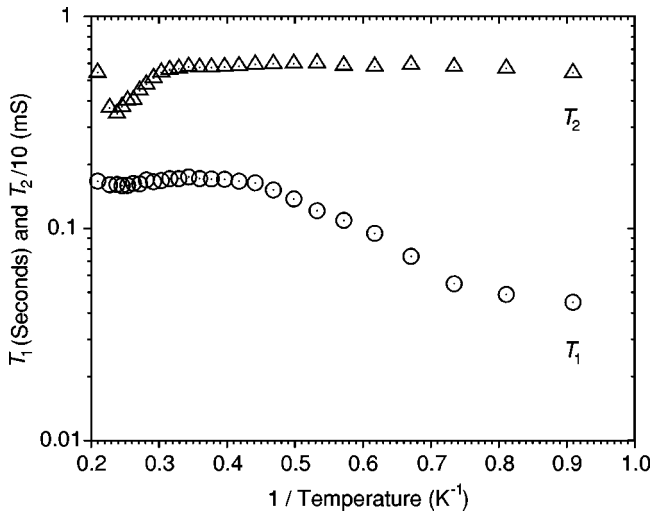

FIG. 3. ^{3}He T_1 and T_2 data as a function of inverse temperature, taken at 0.75 monolayers and 4.5 MHz. The T_2 values have been divided by 10. Incidently, note the sharp dip in T_2 at ~ 3 K, due to relaxation in electronic impurity fields, of the suddenly delocalized ^{3}He spins at the order-disorder phase transition.

There is, however, a serious problem with the assumption of a 4.5 MHz ^{14}N quadrupole frequency—recently this quantity has been measured by three separate groups[14] and is only 210 kHz in stark contrast with other covalently bonded nitrogen compounds where $\omega_Q/2\pi$ is typically $\sim$MHz.[15] We explain the paradox by examining the effects of registered, adsorbed ^{3}He spins on the surface-layer *B* and N electric field gradients (EFG's) *eq* using the *ab initio* full-potential linear augmented plane wave (FLAPW) electronic structure calculation method.[16] The FLAPW method which makes no assumptions about the shape of the charge distribution has proved a highly accurate technique for estimating EFG's which are among the most sensitive and difficult to calculate of crystalline properties and it also provides an invaluable insight into their physical origin.[17] In terms of the LAPW basis the total EFG's at the nuclear centers can be decomposed into *valence* and *lattice* contributions: Contributions from the non-spherical charge distribution inside the atomic spheres are termed *valence* and those from the interstitial region *lattice*. The *valence* contributions can be further decomposed into *p-p*, *d-d*, and *s-d* orbital type terms. The key finding of Blaha *et al.*[17] was that it is the charge inside the first node of the radial wavefunction of the *p-p* term that usually dominates all other EFG contributions. However, the $2p$ radial wave functions of the first-row elements are nodeless causing their tails and EFG contributions to reach far outside their own spheres into the interstitial region and the spheres of adjacent atoms. Table I reveals a substantial negative *lattice* and positive *valence* components giving partial cancellation. For ^{14}N in bare BN a high degree of cancellation occurs explaining the small observed EFG.[14] Using the LDA (see Table I) calculation values and ^{14}N nuclear quadrupole moment $Q=0.019$ b (Bastow *et al.*[14]), $\omega_Q/2\pi = 3e^2qQ/2I(2I-1)h = 283$ KHz and for ^{11}B with $Q=0.041$ b, $\omega_Q/2\pi = 1.49$ MHz. The ^{11}B value is in excellent agreement with experiment, the ^{14}N rather less so. The bare BN GGA (see Table I) ^{14}N *valence* EFG is 18% less than in the LDA calculation and demonstrates its abnormally

TABLE I. Decomposition of the EFG's in *h*-BN and for comparison, graphite; for bare substrates and with a helium adatom, using LDA (local density approximation) and GGA (generalized gradient approximation) treatments for exchange and correlation (EC) (see Ref. 16 and references therein for details). EFG Units are 10^{21} V/m^2. Note 1: For computational simplicity 1 adatom per unit cell, inserted in the layer was used. Note 2: For graphite only the first inequivalent C atom, C_1 is shown.

System	EC	Atom	Total	Valence	Lattice
bare BN	LDA	N	0.41145	2.2914	−1.8799
bare BN	LDA	B	3.0412	3.9069	−0.8658
bare BN	GGA	N	−0.0212	1.8647	−1.8860
bare BN	GGA	B	3.0515	3.8877	−0.8362
BN+adatom	LDA	N	3.1730	5.3510	−2.1780
BN+adatom	LDA	B	3.1001	4.2742	−1.1741
BN+adatom	GGA	N	2.6989	4.8794	−2.1805
BN+adatom	GGA	B	3.0875	4.2283	−1.1409
bare graphite	LDA	C_1	3.0119	4.7055	−1.6936
bare graphite	GGA	C_1	2.8377	4.5248	−1.6871
graphite+adatom	LDA	C_1	2.9020	5.0095	−2.1076
graphite+adatom	GGA	C_1	2.7007	4.7966	−2.0959

high sensitivity to the treatment of exchange and correlation, resulting in near total cancellation. For B and C in graphite the reductions are only 0.5 and 3.8% and are typical of FLAPW calculations. Insertion of a helium adatom increases the N *valence* EFG by 134% (LDA calculation) but those of B and C in graphite by only 9 and 6.5%, respectively, the cancellation effect raising the total N EFG by 670% while leaving the B value essentially unchanged. The corresponding ^{14}N $\omega_Q/2\pi$ is 2.2 MHz, which given the extreme sensitivity demonstrated for the N EFG is plausibly within range of our 4.5 MHz hypothesis. The adatom's 1*s* electrons do not contribute directly to the EFG's but do displace the polarizable N-*p* charge leading to the observed results in the surface-layer ^{14}N atoms.

Below 1.5 K, at $x=0.75$ large negative deviations from Curie's law in ^{3}He magnetic susceptibility are apparent which is another indication of tightly coupled ^{3}He-substrate spin systems and has been extensively reported in magnetic saturation experiments between ^{19}F and ^{3}He on the surface of the 0.2 μm fluorocarbon polymer beads of the DLX6000 lubricant powder.[18] Assuming saturated substrate spins and applying the simple direct coupling model[18] to each ^{3}He *substrate spin* system allows the maximum attainable decrease in ^{3}He susceptibility, labeled *R*, to be estimated. Our experimental value $R=0.69\pm0.05$ shows interior ^{11}B spins, which have the largest magnetic moment form the dominant contribution. Achieving significant saturation requires a short intracrystalline spin-diffusion time $T_{SD}\lesssim$ the experimental pulse recycle rate—i.e., seconds but for a typical, e.g., 5 μm, regular BN particle, $T_{SD}\sim 1$ h. However, knowing the crystallites to be flat in shape with 5% of the surface being edge-area we have modeled the particles as flat square slabs. This leads to an average particle with basal plane dimensions of 4.7 μm and slab thickness 0.12 μm, which compares with the DLX6000 bead radius. Refreshed via ^{3}He on the basal planes, the magnetization need only diffuse a distance $\sim\frac{1}{2}\times 0.12$ μm to reach the crystallites interiors, giving $T_{SD}\sim 2$ s. Clearly an effective magnetization sink, it fulfills condition (3) above.

Throughout this work we fitted spin-echo data to the phenomenological stretched-exponential function $h(\infty)-h(t)=h(0)\exp-(t/T_1)^{\beta}$. The *index* of relaxation β turns out to be a very sensitive indicator of phase and relaxation-pathway changes in the film, particularly in the temperature data for $x<0.75$ where it provides an indication of the registered spin population. Figure 1(b) shows that *glassy-solid* type subexponential relaxation (i.e., $\beta<1$) gives way to a large superexponential (SE) peak at registry. Increasing β at 4.5 MHz is the most sensitive indicator of the presence of registered spins and ^{14}N coupled relaxation. We have no clear-cut explanation for this effect. Instead, we list some potentially relevant points: (a) On an exponential basis, SE relaxation is equivalent to the instantaneous relaxation rate increasing with time. As time increases the ^{3}He magnetization recovery is sourced from progressively further inside the crystallites and via multiple surfaces. (b) The EFG modifications induced by the adatoms may be time-varying due to ^{3}He exchange motion with implications for quadrupolar relaxation. (c) At the QD, *long-tailed* surface dipolar correlation functions can lead to SE relaxation for sufficiently slow motion and strong coupling. See T_2 treatment in Ref. 19. (d) As an experimental artifact, the magnetization depression effect might cumulatively produce an apparent extra relaxation contribution as measurements proceeded.

To conclude, our observation of strong ^{3}He–^{14}N (surface-layer)–^{11}B (subsurface) coupled relaxation on the homogeneous *h*-BN surface at 4.5 MHz has revealed a useful new tool for investigations of specifically, the commensurate phases (e.g., fluid-commensurate coexistences, exotic low temperature commensurate and striped phases) of spin-bearing quantum adsorbates on *h*-BN and possibly also new materials such as BN nanotubes or fullerene analogs. The huge sensitivity of the polarizable surface nitrogen EFG, even to small, low-polarizability adatoms is remarkable and possibly unique to BN substrates.

[1] R.S. Pease, Acta Crystallogr. **5**, 356 (1952).
[2] J. Regnier, A. Thomy, and X. Duval, J. Colloid Interface Sci. **70**, 74 (1979).
[3] J. Zupan, M. Komac, and D. Kolar, J. Appl. Phys. **41**, 5337 (1970).
[4] N. Ganguli and K.S. Krishman, Proc. R. Soc. London, Ser. A **177**, 168 (1941).
[5] T. Crane and B. Cowan, Physica B **194**, 633 (1994); **284**, 230 (2000).
[6] A. Abragam, *The Principles of Nuclear Magnetism* (Oxford University Press, Oxford, 1986).
[7] F. Winter and R. Kimmich, Mol. Phys. **45**, 33 (1982).
[8] F. Winter and R. Kimmich, Biochim. Biophys. Acta **719**, 292 (1982); R. Kimmich, F. Winter, W. Nusser, and K.-H. Spohn, J.

Mater. Res. **68**, 263 (1986); D. Stephenson and J.A.S. Smith, Proc. R. Soc. London, Ser. A **416**, 149 (1988); M.H. Palmer, M.M.P. Kurshid, T.J. Rayner, and J.A.S. Smith, Chem. Phys. **182**, 27 (1994).

[9] F. Noack, Prog. Nucl. Magn. Reson. Spectrosc. **18**, 171 (1986).

[10] A.H. Silver and P.J. Bray, J. Chem. Phys. **32**, 288 (1960); M.B. Khusidman and V.S. Neshpor, Zh. Strukt. Khim. **12**, 1094 (1971) [J. Struct. Chem. **12**, 1008 (1971)]; C. Connor, J. Chang, and A. Pines, Rev. Sci. Instrum. **61**, 1059 (1990); P.S. Marchetti *et al.*, Chem. Mater. **3**, 482 (1991).

[11] F.W. van Keuls, T.J. Gramila, L.J. Friedman, and R.C. Richardson, Physica B **165-166**, 717 (1990).

[12] P.-O. Westlund and H. Wennerström, J. Magn. Reson. **63**, 280 (1985).

[13] B. Cowan, L.A. El-Nasr, and M. Fardis, Jpn. J. Appl. Phys., Suppl. **26**, 307 (1987).

[14] T.J. Bastow, D. Massiot, and J.P. Coutures, Solid State Nucl. Magn. Reson. **10**, 241 (1998); J. Jeschke, W. Hoffbauer, and M. Jansen, *ibid.* **12**, 1 (1998); T. Minamisono *et al.*, Z. Naturforsch., A: Phys. Sci. **53**, 293 (1998).

[15] I. P. Biryukov, M. G. Voronkov, and A. Safin, *Tables Of Nuclear Quadrupole Resonance Frequencies* (Daniel Davey and Co., New York, 1969).

[16] P. Blaha, K. Schwarz, and J. Luitz, WIEN97, *A Full Potential Linearized Augmented Plane Wave Package for Calculating Crystal Properties*, 1999; P. Blaha, K. Schwarz, P. Sorantin, and S.B. Trickey, Comput. Phys. Commun. **59**, 399 (1990).

[17] P. Blaha, R. Sorantin, C. Ambrosch, and K. Schwarz, Hyperfine Interact. **51**, 917 (1989); K. Schwarz and P. Blaha, Z. Naturforsch., A: Phys. Sci. **47**, 197 (1991).

[18] L.J. Friedman, T.J. Gramila, and R.C. Richardson, J. Low Temp. Phys. **55**, 83 (1984); A. Schuhl, F.B. Rasmussen, and M. Chapellier, *ibid.* **57**, 483 (1984); A. Schuhl, S. Maegawa, M.W. Meisel, and M. Chapellier, Phys. Rev. B **36**, 6811 (1987); Q. Geng, M. Olsen, and F.B. Rasmussen, J. Low Temp. Phys. **74**, 369 (1989).

[19] B.P. Cowan, J. Phys. C **13**, 4575 (1980).